RSC Advances

ROYAL SOCIETY OF CHEMISTRY

www.rsc.org/advances

A table of contents entry

Non-woven polypropylene supported bovine serum albumin imprinted calcium alginate/polyacrylamide hydrogel film with good regeneration performance.

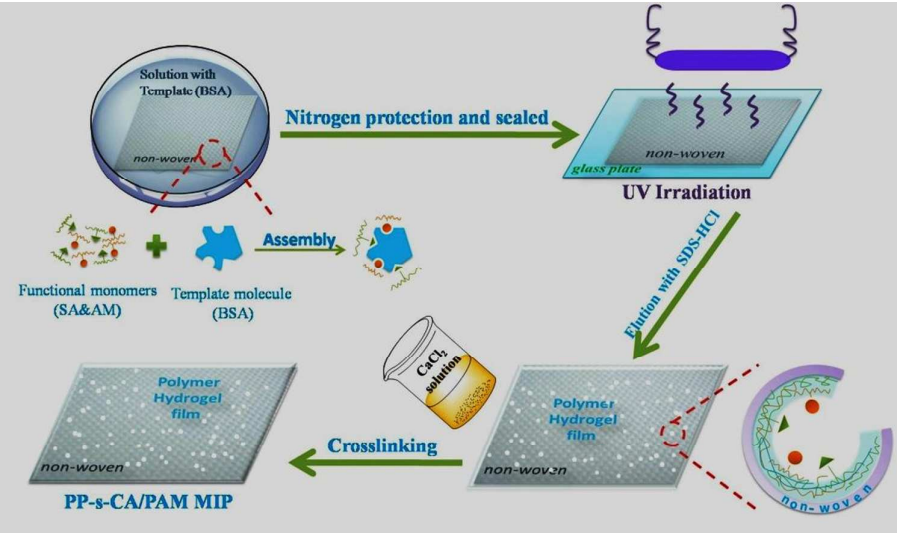

Fig. 1. Schematic representation of preparing non-woven polypropylene supported BSA imprinted calcium alginate/polyacrylamide hydrogel film with good regeneration performance.

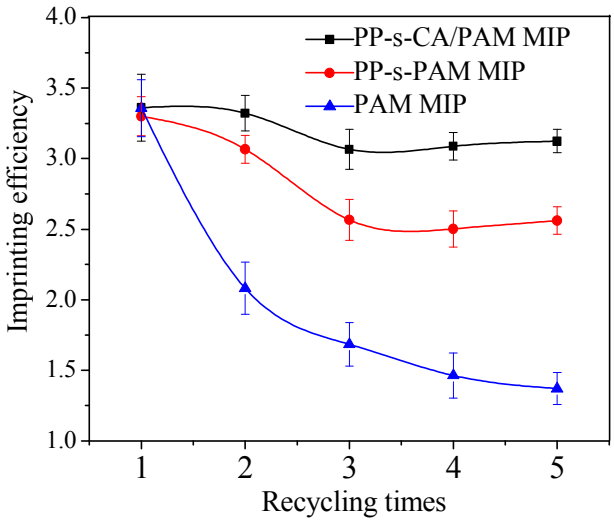

Fig. 2. Curves of the regeneration properties of PP-s-CA/PAM MIP, PP-s-PAM MIP and PAM MIP.

RSC advances RSCPublishing

ARTICLE

Imprinting of bovine serum albumin in nonwoven polypropylene membrane supported polyacrylamide/ calcium alginate interpenetrating polymer network hydrogel

Cite this: DOI: 10.1039/x0xx00000x

Received 00th January 2012,
Accepted 00th January 2012

DOI: 10.1039/x0xx00000x

www.rsc.org/

Bohong Kan[a], Beibei Lin[b], Kongyin Zhao[b,c]*, Xinxin Zhang[b], Lingzhi Feng[b], Junfu Wei[b,c] and Yingchang Fan[a]

Abstract: Bovine serum albumin (BSA) imprinted nonwoven polypropylene (PP) fibre supported calcium alginate/polyacrylamide (CA/PAM) hydrogel film (PP-s-CA/PAM MIP) was prepared using nonwoven PP as matrix, BSA as template molecule, sodium alginate (SA) and acrylamide (AM) as functional monomers, N, N′-methylenebisacrylamide (MBA) as covalent cross-linker, and $CaCl_2$ as ionic cross-linker by UV radiation-reduced polymerization in an aqueous phase. Factors affecting the adsorption capacity and imprinting efficiency of the BSA-imprinted PP-s-CA/PAM MIPs were investigated. The results showed that PP-s-CA/PAM MIPs exhibited an obvious improvement in terms of adsorption capacity and recognition for BSA compared with the non-imprinted ones. The adsorption capacity of MIP for BSA reached 27.02 mg/g when the adsorption time was 900min, which was 2.8 times of the non-imprinted one. The swelling of CA/PAM hydrogel supported on PP was significantly reduced. In addition, the regeneration property of BSA-imprinted PP-s-CA/PAM hydrogel was distinctly improved. The imprinting efficiency of PP-s-CA/PAM MIP maintained at 92.95% of the initial value even after five repetitions.

1. Introduction

Molecular imprinting is a useful technique for forming complementary binding sites by copolymerizing suitable functional monomers in the presence of suitable template molecules [1,2]. Molecularly imprinted polymers (MIPs) are characterized by their thermal and chemical stability, high specificity, ease of mass preparation, low cost and reusability. MIPs have been used in various applications including separation [3–4], solid-phase extraction [5], catalysis [6], biomimetic sensor [7], and drug delivery [8]. Although molecular imprinting has been successfully applied in imprinting low-molecular weight compounds [9,10], the imprinting of bio-macromoleculars in particular proteins was still a significant challenge due to the inherent technical problems [11,12]. Proteins are usually instable and insoluble and can be easily affected by temperature or other environment factors.

Polyacrylamide (PAM) hydrogels can be easily produced and have been identified as suitable imprinting matrices for biological molecules [13–20]. However, PAM hydrogels have poor regeneration property because of their soft texture [17]. It is difficult for the mass transfer of proteins in PAM bulk hydrogels. Surface imprinting protocols can eliminate the problems associated with mass transfer [18, 19]. Lu et al.[20] fabricated BSA and lysozyme surface-imprinted magnetic gel microspheres by using magnetic composite gel microspheres as seeds via inverse-phase seed suspension polymerization. Qin et al.[21] fabricated lysozyme imprinted polymer beads by using chloromethylated polystyrene beads as supports via surface-initiated living radical polymerization in aqueous media. Guo et al.[22, 23] prepared bovine haemoglobin imprinted chitosan microspheres by trapping selective soft PAM gel in the pores of the cross-linked chitosan beads.

Almost all protein-imprinted PAM hydrogels are particles or microspheres and organic solvents are often used as dispersion medium, which inevitably causes protein denaturation. Films have more advantages than microspheres or granules in biological applications such as cell culture. However, it is difficult to obtain PAM hydrogel thin films. Protein molecularly imprinted alginate film was prepared using an aqueous imprinting method without any organic chemicals, which was favourable in life science applications such as medical devices, food additives, or drug delivery systems [24]. Suo et al. [25] synthesized highly stretchable and tough hydrogels from sodium alginate (SA) and acrylamide (AM). The hybrid hydrogels may exhibit good performance in maintaining the imprinted cavities

[a] First Teaching Hospital of Tianjin University of Traditional Chinese Medicine, Tianjin 300193, China.
[b] State Key Laboratory of Hollow Fibre Film Materials and Processes, Tianjin Polytechnic University, Tianjin 300387, China.
[c] School of Material Science and Engineering, Tianjin Polytechnic University, Tianjin 300387, China
Corresponding author: E-mail: tjzhaokongyin@163.com, Tel.: +086 -022 83955362, Fax, +086 -022 8395055

and improving the regeneration property of the MIPs. In our previous work, bovine serum albumin (BSA) imprinted polypropylene (PP) fibre-grafted polyacrylamide hydrogel was prepared using non-woven PP fibre as matrix, BSA as template molecule, and acrylamide as functional monomer. The imprinting efficiency of MIP maintained at 76% of the initial value even after five repetitions [26]. However, the adsorption capacity of the MIP was low, and the strength of the PAM hydrogel was poor.

In this paper, BSA imprinted nonwoven PP fibre supported calcium alginate/polyacrylamide (PP-s-CA/PAM MIP) hydrogel film was prepared by UV radiation-reduced polymerization using PP as matrix, BSA as template, SA and AM as functional monomers, N,N′-methylenebisacrylamide (MBA) and $CaCl_2$ as crosslinkers. The swelling of CA/PAM hydrogel supported on nonwoven PP was reduced and the regeneration property of BSA imprinted PP-s-CA/PAM hydrogel was distinctly improved. Factors affecting the adsorption capacity and imprinting efficiency of PP-s-CA/PAM MIPs were investigated. The adsorption capacity of MIP reached 27.02 mg/g, which was 2.8 times of the non-imprinted ones. The MIPs can be easily prepared and applied in protein analysis and testing, cell culture, as well as the controlled release and separation of proteins.

2. Experimental

2.1 Materials

Nonwoven PP fibre (22 g/m^2) were purchased from Xianghehuaxin Nonwoven Company, Ltd. (Langfang, China). SA was purchased from Tianjin Yuanhang chemical company. Acrylamide (AM) and MBA were analytical reagents and purchased from Chemistry Reagent Factory of Tianjin (Tianjin, China). Acetic acid (HAc), sodium dodecyl sulfate (SDS), and ammonium persulfate (APS) were obtained from the Institute of Tianjin Guangfu Fine Chemicals (Tianjin, China). BSA, ovalbumin (Ova), bovine hemoglobin (Hb), Lysozyme (Lyz), and bovine γ-globulin (Glo) were purchased from Lanji of Shanghai Science and Technology Development Company (Shanghai, China).

2.2 Preparation of PP-s-CA/PAM MIP

Fig. 1 shows the schematic representation of the fabrication procedure of the BSA-imprinted PP-s-PAM/CA. Nonwoven PP fibre (640 mg) was introduced into 30 mL aqueous solution consisting of BSA (45 mg), AM (3 g), APS (30 mg), MBA (2.4 mg) and SA (150 mg). The mixture was then incubated for 1 h at room temperature for the pre-assembly between the template molecules and functional monomers. The nonwoven PP fibres immersed in the mixture were transferred into quartz glass sheet, purged with nitrogen for 8 min, and then sealed. Then the polymerization was conducted for 0.5 h by UV irradiation at room temperature to produce the polymer hydrogel. The hydrogel supported on nonwoven PP fibres were rinsed repeatedly with distilled water to remove unreacted monomers and crosslinkers. The protein in the hydrogel was eluted with HAc solution (10%, v/v) containing SDS (10%, w/v) until no BSA in the supernatant was detected by measuring the UV absorbance at 280 nm. The nonwoven PP supported hydrogel was then extensively washed with deionized water to remove the remnant SDS and HAc. Then the hydrogel supported on nonwoven PP was cross-linked with 2.5% $CaCl_2$ to obtain PP-s-CA/PAM MIP.

Nonwoven PP supported non-imprinted CA/PAM (i.e., PP-s-CA/PAM NIP) was also prepared using the same procedures but without the template.

2.3 Preparation of PP-g-PAM MIP and PAM MIP

BSA imprinted nonwoven PP fibre supported polyacrylamide hydrogel film (PP-g-PAM MIP) and polyacrylamide (PAM) hydrogel microspheres (PAM MIP) were prepared according to the literature [27-30]. The non-imprinted hydrogels (i.e., PP-g-PAM NIP and PAM NIP) were also prepared using the same procedure but without the template.

2.4 Characterization

The morphologies of PP and PP-s-CA/PAM MIP were observed using a scanning electron microscope (FESEM; S-4800, HITACHI, Japan).

The thickness of wet CA/PAM hydrogel was measured with a digital display micrometer gauge from Shanghai Luchuan co., LTD.

2.5 Swelling performance

Water on the surface of wet CA/PAM and PP-s-CA/PAM was removed using a filter paper, and the weight of the wet hydrogels was measured. The CA/PAM and PP-s-CA/PAM were soaked in normal saline (0.9 wt.% NaCl), and the mass of the hydrogels was measured at time t. The swelling ratio (SR) of CA/PAM and PP-s-CA/PAM under different time is defined as follows:

$$SR=(W_t - W_w)/W_w \quad (1),$$

where W_w and W_t are the weight of the wet hydrogel before and after swelling at time t, respectively. The weight of the nonwoven PP wasreduced from that of the PP-s-CA/PAM in the swelling degree calculation.

2.6 Adsorption experiments

Surface water on the wet PP-s-CA/PAM MIPs or NIPs was absorbed using filter paper. Subsequently, 1.0 g of wet PP-s-CA/PAM MIPs or NIPs were added in each glass bottle containing 10 mL BSA solutions (1.36 mg/mL) to evaluate the imprinting efficiency and dynamic adsorption or various BSA concentrations (0 mg/mL to 3.0 mg/mL) to determine the adsorption isotherms. At certain intervals, the supernatant solutions were collected and determined with a UV spectrophotometer. The experiments were carried out for three times and the averages of the results were used. The equilibrium adsorption capacity Q_e (mg/g) of the protein adsorbed was calculated according to the following equation:

$$Q_e = (C_0 - C_e)\, V/W \quad (2),$$

where W (g) is the mass of the dried MIPs or NIP, V (ml) is the volume of the BSA solution, C_0 and C_e are the initial and final BSA concentrations at equilibrium, respectively. The imprinting efficiency (IE) of MIPs was defined as the following equation: [27-30].

$$IE = Q_{MIP}/Q_{NIP} \quad (3),$$

where Q_{MIP} and Q_{NIP} are the Q_e of MIPs and NIPs, respectively.

Dynamic adsorption capacity Q_t at time t was calculated according to the following equation:

$$Q_t = (C_0 - C_t)\, V/W \quad (4),$$

where C_t (mg/mL) is the BSA concentration in the supernatant at time t.

2.7 Recognition performance

Wet PP-s-CA/PAM MIPs or NIPs (0.5 g) were placed into each glass bottle containing 10 mL of 1.36 mg/mL different protein solutions for 24h to evaluate the recognition performances. The recognition performance of MIPs can be evaluated by the static distribution coefficient K_D, the separation factor α and the relative separation factors β, which are defined in the following equations:

$$K_D = C_P/C_S \quad (5)\ [31\text{-}33],$$

where C_p is the concentration of protein on wet gel, and C_S is the concentration of protein in the solution.

$$\alpha = K_{D1}/K_{D2} \quad (6),$$

where K_{D1} and K_{D2} are the static distribution coefficients of the template and other competitive proteins, respectively.

The relative separation factors β was introduced and defined as follows:

$$\beta = \alpha_I/\alpha_N \quad (7),$$

where α_I and α_N are the separation factors of the template on MIPs and NIPs.

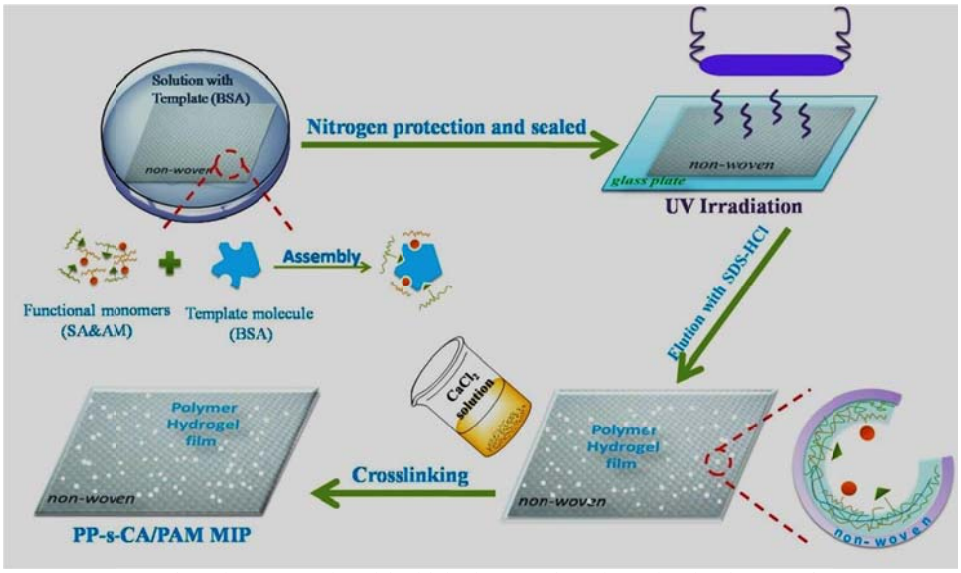

Fig. 1. Schematic representation of the fabrication procedure of BSA-imprinted PP-s-CA/PAM.

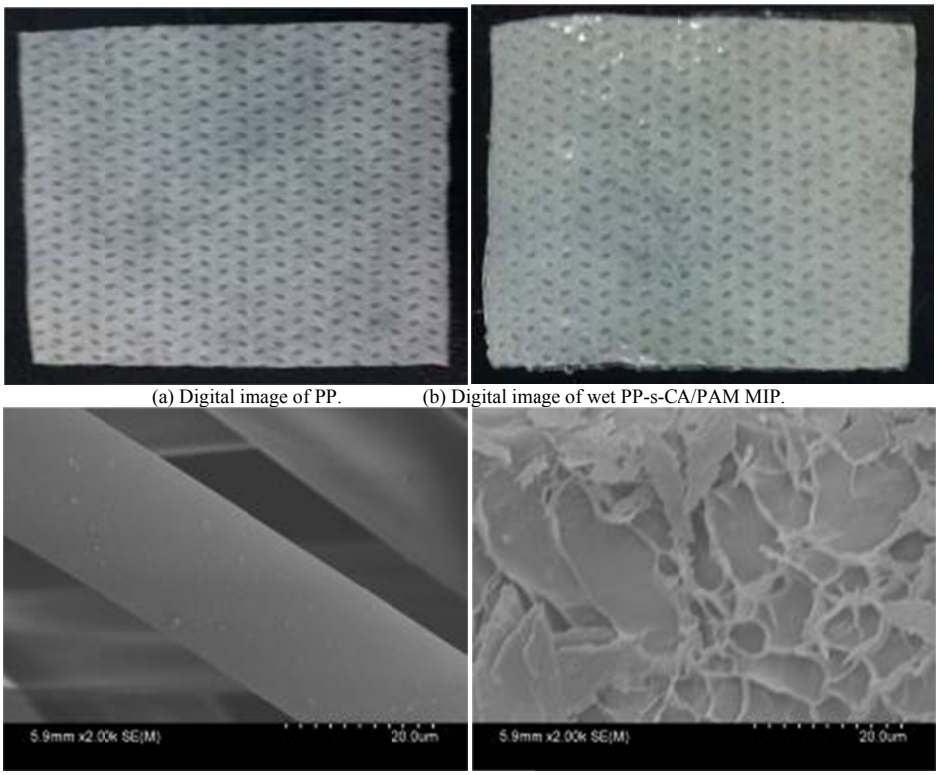

(a) Digital image of PP. (b) Digital image of wet PP-s-CA/PAM MIP.

(c) SEM image of PP. (d) SEM image of PP-s-CA/PAM MIP.

Fig. 2. Digital (wet) and SEM images of nonwoven PP and PP-s-CA/PAM MIP.

3 Results and discussions

3.1 Surface morphology

Fig. 2 shows the digital (wet) and SEM images of the nonwoven PP and PP-s-CA/PAM MIP. The wet CA/PAM was transparent with a thickness of approximately 0.23 mm. Significant lamellar macroporous structure was found on the surface of PP-s-CA/PAM MIP (Fig. 2(d)). The macroporous structure on the surface of

CA/PAM hydrogel facilitated the diffusion of the protein template. Imprinting pores were not found because they were too small and the water evaporation in vacuum resulted in pore shrinkage.

3.2 Factors affecting Q_e and *IE* of MIP

The effects of different MBA concentrations on the Q_e and *IE* of PP-s-CA/PAM MIP are shown in Fig. 3. The adsorption of BSA on MIP increased gradually with the initial increase in MBA concentration, and then decreased rapidly when MBA concentration ≥0.08 wt.%. At low MBA concentration, Q_e was also low because MIP is too weak to maintain the imprinted cavities. By contrast, the Q_e of MIP decreased when MBA concentration ≥0.08 wt.% because excessively crosslinked PP-s-CA/PAM hydrogel hindered protein diffusion. *IE* reached its maximum value when the proportion of MBA was 0.08 wt.%.

The effects of monomer concentration on the Q_e and *IE* of MIP are shown in Fig. 4. The Q_e of MIP and NIP both increased with the increase in monomer concentration from 5 wt.% to 10 wt.%. The Q_e values of BSA on both MIP and NIP reached their maximum values when the monomer concentration was 10 wt.%. The BSA adsorption on MIP was significantly higher than that of NIPs at low monomer concentration. The Q_e of MIP and NIP decreased when the monomer concentration was >10 wt.%. When the monomer concentration was 5 wt.%, *IE* reached its maximum value (2.65). At low monomer concentration (<10 wt.%), the increase in monomer concentration resulted in an increase in Q_e of BSA on MIPs because more imprinting cavities were created. However, the adsorption of BSA on MIPs decreased when the monomer concentration was above 10%, which was attributed to the difficulty in the absolute removal of the templates from the hydrogel matrix.

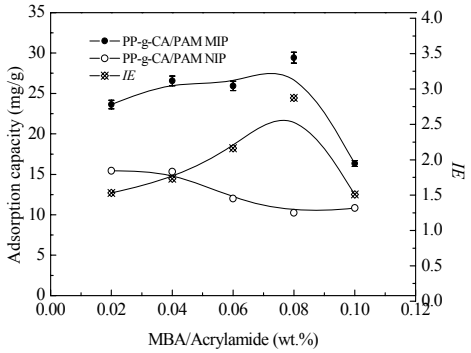

Fig. 3. Effects of different MBA concentrations on the Q_e and *IE* of PP-s-CA/PAM MIP and NIP. Monomer concentration was 10 wt.%; SA concentration was 0.5 wt. %.

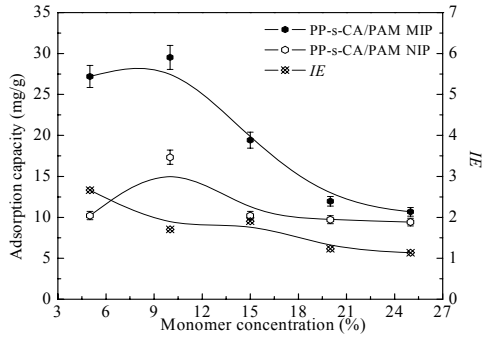

Fig. 4. Effects of monomer concentration on the Q_e and *IE* of PP-s-CA/PAM MIP and NIP. SA concentration was 0.5 wt. %; MBA/Acrylamide=0.08 wt. %.

SA concentration showed critical effect on the Q_e and *IE* of PP-s-CA/PAM MIP. Fig. 5 shows that MIP had maximum Q_e and *IE* values when the concentration of SA was 0.5 wt.%. Initially, the adsorption of BSA on MIP rapidly increased with the increase in SA. The Q_e of protein decreased gradually when the concentration of SA was above 0.5 wt.%. At low SA concentration, the increase in Q_e was attributed to the formation of alginate/PAM interpenetrating network, which increased the number of imprinted cavities. In addition, the carboxylate anion of alginate interacted with amino in BSA, which was beneficial for the adsorption of BSA. However, the space mesh of the hydrogel was reduced when SA concentration >0.5 wt.%, which hindered mass transfer of BSA, causing the decrease in Q_e.

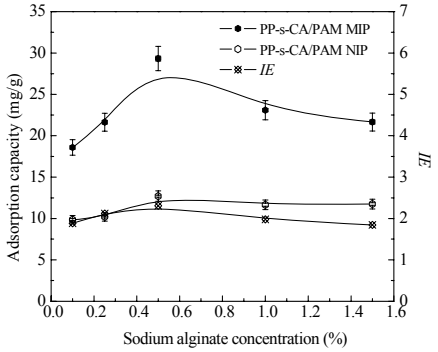

Fig. 5. Effects of SA concentration on the Q_e and *IE* of PP-s-CA/PAM MIP and NIP. Monomer concentration was 10 wt. %, MBA/Acrylamide =0.08 wt. %.

3.3 Adsorption kinetics

The adsorption dynamic curves of PP-s-CA/PAM MIP and NIP are shown in Fig. 6. MIP adsorbed more BSA than NIP, and the Q_e of MIP was almost three times of that of NIP. An abrupt increase in the adsorption capacity of MIP was observed during the first 360 min, and the adsorption capacity almost reached equilibrium after 900 min. At the beginning, a large number of imprinted cavities exposed on the surface of MIP, and the template easily reached the specific binding sites, resulting in high *IE* of the MIP. When the superficial imprinting sites were filled up, the adsorption rate declined and the *IE* of MIP decreased.

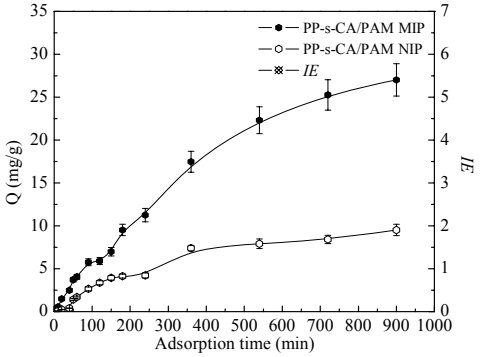

Fig. 6. Adsorption kinetic curve.

3.4 Adsorption thermodynamic

Fig. 7 shows the thermodynamic adsorption curves of PP-s-CA/PAM MIP and NIP. The Q_e of MIP increased gradually at low BSA concentrations because the amount of BSA was insufficient to fill up the specific binding cavities. However, almost all specific

imprinted sites were gradually occupied and the Q_e of MIPs became steady with the increase in BSA concentration. PP-s-CA/PAM MIPs showed higher adsorption capacity for BSA than NIPs.

3.5 Regeneration properties

After BSA absorption, the PP-s-CA/PAM MIP was washed with 10% (v/v) acetic acid containing 1% (w/v) SDS to remove BSA, and then was applied to re-adsorb BSA. The imprinting reproducibility of MIP was examined for several repeated adsorption–regeneration cycles, and the regeneration property of BSA-imprinted PAM hydrogel bead was also investigated [27]. The *IE* of PP-s-CA/PAM MIP decreased more slowly than those of PP-g-PAM MIP and PAM MIP and was maintained at 92.95% of the initial value even after five cycles (Fig. 8). However, the *IE* of the BSA-imprinted PAM microspheres declined with the increase of cycle times; the imprinting effect almost disappeared after five cycle times. The soft texture of the PAM gel microspheres cannot stabilize the shape of the binding sites. By contrast, the strength of PP-s-CA/PAM was significantly improved and the shape of the binding sites was stabilized. In addition, the swelling of CA/PAM hydrogel supported on nonwoven PP was significantly reduced (Fig. 9). A 0.9 % NaCl solution was used for swelling performance because 0.9% NaCl solution is often used in cell culture, protein adsorption and release in simulated body fluids. CA/PAM hydrogel remarkably swelled because the Ca^{2+} in CA/PAM hydrogel was replaced by Na^{+} in physiological saline. The *SR* of CA/PAM hydrogel reached 42.94% after 300 min. However, the *SR* of nonwoven PP supported CA/PAM hydrogel almost reached equilibrium after 20 min, with a value of 8.67%. Thus, PP-s-CA/PAM maintained the imprinted cavities without distortion better than PAM and CA/PAM.

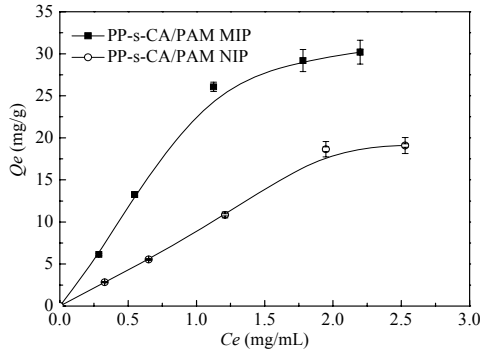

Fig. 7. Thermodynamic adsorption curves of PP-s-CA/PAM MIP and NIP. Monomer concentration was 10 wt. %, SA concentration was 0.5 wt. %, and MBA/Acrylamide =0.08 wt. %.

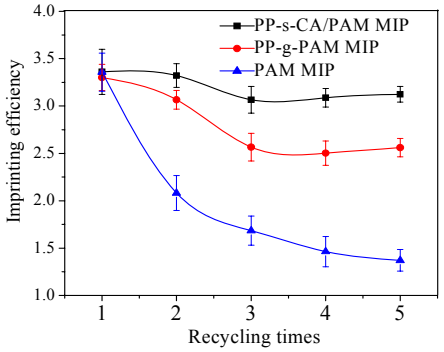

Fig. 8. Curves of the regeneration properties of PP-s-CA/PAM MIP, PP-g-PAM MIP and PAM MIP.

3.6 Recognition performance

Table 1 shows the Q_e, α, and β values of PP-s-CA/PAM MIP and NIP for BSA and competitive proteins. MIP exhibited good adsorption selectivity for BSA template. The Q_e of BSA on MIP was higher than those of Lyz, Ova, Hb, and Glo. The α and β of BSA-imprinted PP-s-CA/PAM increased with the increase in protein M_w, except for HB. The higher BSA affinity of MIP is attributed to the generation of BSA high-affinity adsorption sites and the complementary cavities in the hydrogel during polymerization. Thus, the template protein was strongly bound to the MIP. For the competitive proteins, although Lyz was small enough to diffuse into the imprinting cavities, it had less chance to be adsorbed on the PP-s-CA/PAM MIP because it was not complementary with the recognition sites. The Q_e of γ-Glo on MIP was significantly lower than that of any protein because the molecular volume of γ-Glo was remarkably larger than those of other proteins. PP-s-CA/PAM NIP showed lower Q_e for BSA than MIP, which is attributed to the failure of NIP to form specific recognition sites because of the absence of template BSA. As basic proteins, Lyz and Hb showed more favorable interactions with PP-s-CA/PAM, thereby causing non-specific adsorption and poor adsorption selectivity. Larger protein such as Glo was likely to be excluded from the binding cavities, which resulted in lower Q_e and higher α and β values.

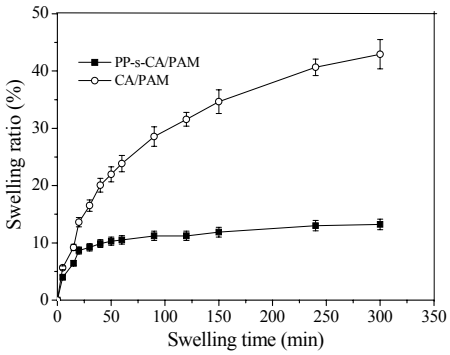

Fig. 9. Swelling ratio of PP-s-CA/PAM and CA/PAM in 0.9 wt.% NaCl solution under different time.

Table 1 Q_e, α and β values of BSA-imprinted and non-imprinted PP-s-CA/PAM.

Protein properties			$Q_{e(MIP)}$	$Q_{e(NIP)}$	α_{MIP}	α_{NIP}	β
	Mw (kDa)	pI	BSA MIP	NIP	BSA MIP	NIP	--
Lyz	15	10.5	17.71 ±0.99	14.50 ±0.84	1.611 ±0.12	0.549 ±0.03	2.94 ±0.19
Ova	43	4.7	9.17 ±0.73	10.37 ±0.71	3.177 ±0.18	0.774 ±0.05	4.11 ±0.22
Hb	64	6.9	9.36 ±0.56	6.05 ±0.45	3.103 ±0.22	1.338 ±0.08	2.32 ±0.12
BSA	67	4.9	27.02 ±1.54	9.52 ±0.75	--	--	--
Glo	160	7.1	5.09 ±0.32	4.94 ±0.36	5.762 ±0.35	1.652 ±0.096	3.49 ±0.25

4. Conclusions

BSA-imprinted PP fibre supported CA/PAM hydrogel film was successfully synthesized by UV radiation-reduced polymerization using nonwoven PP fibre as matrix, BSA as template, SA and AM as functional monomers, MBA as covalent crosslinker, and $CaCl_2$ as ionic crosslinker. The swelling of PP-s-CA/PAM NIP was significantly reduced.

Analyses of the adsorption dynamics and isotherms showed that the PP-s-CA/PAM MIP exhibited significant improvement in adsorption capacity for BSA compared with NIP. The PP-s-CA/PAM MIP recognized the template protein, which was confirmed using Lyz, Ova, Hb, and Glo as control proteins; The selectivity factor (β) was above 2.3. The imprinting efficiency of PP-s-CA/PAM MIP was maintained at 92.95% of the initial value even after five repetitions. PP-s-CA/PAM maintained the imprinted cavities without distortion better than PAM and CA/PAM.

PP-s-CA/PAM MIP is low cost and can be easily prepared and applied in protein analysis and testing, cell culture, as well as controlled release and the separation of proteins.

Acknowledgements

The research is supported by the National Natural Science Foundation of China (51103102, 81173413), Ministry of education doctoral new teacher fund (20111201120004), and the Tianjin Colleges Science and Technology Development Fund (20100308, 20120211).

References

1 Z. Zhang, L.X. Chen, F.F. Yang and J.H. Li, *Rsc Adv.,* 2014, **4**, 31507.
2 S.J. Li, S.S. Cao, M.J. Whitcombe and S.A. Piletsky, *Prog. Polym. Sci*., 2014, **39**, 145–163.
3 W. Rao, R. Cai, Z.H. Zhang, Y.L. Yin, F. Long and X.X. Fu, *Rsc Adv*., 2014, **4**, 18503.
4 Z.Y. Xu, J.F. Wan, S. Liang and X.J. Cao, *Biochem. Eng. J*., 2008, **41**, 280.
5 M. Lasáková and P. Jandera, *J. Sep. Sci*., 2009, **32**, 799.
6 K.Y. Zhao, L.Z. Feng, H.Q. Lin, Y.F. Fu, B.B. Lin, W.K. Cui, S.D. Li, J.F. Wei, *Catal. Today*, 2014, **8**: 127.
7 E. Roy, S.K. Maity, S. Patra, R. Madhuri and P.K. Sharma, *Rsc Adv*., 2014, **4**, 32881.
8 P. Wang, A.X. Zhang, Y. Jin, Q. Zhang, L.Y. Zhang, Y. Peng and S.H. Du, *Rsc Adv*., 2014, **4**, 26063.
9 A. Mirmohseni, M. Shojaei and R. Pourata, *Rsc Adv*., 2014, **4**, 20177.
10 G.Z. Kyzas, D.N. Bikiaris and N.K. Lazaridis, *Chem. Eng. J*., 2009, **149**, 263.
11 N. Sankarakumar and Y.W. Tong, *Rsc Adv*., 2013, **3**, 1519.
12 M. Anda and A. Denizli, *Rsc Adv*., 2014, **4**, 31130.
13 D.M. Hawkins, D. Stevenson and S. Reddy, *Anal. Chim. Acta*., 2005, **542**, 61.
14 S.J. Hjerten, J.L. Liao and K. Nakazato, *Chromatographia*, 1997, **44**, 227.
15 T.Y. Guo, Y.Q. Xia, J. Wang and M.D. Song, B.H. Zhang, *Biomaterials*, 2005, **26**, 5737.
16 G.Q. Fu, J. Zhao, H. Yu, L. Liu and B. He, *React. Funct. Polym*., 2007, **67**, 442–450.
17 X.S. Pang, G.X. Cheng, R.S. Li, S.L. Lu and Y.H. Zhang, *Anal. Chim. Acta*., 2005, **550**, 13.
18 E. Verheyen, J.P. Schillemans, M. Wijk, M.A. Demeniex, W.E. Hennink and C.F. Nostrum, *Biomaterials*, 2011, **32**, 3008.
19 L. Qin, X.W. He, W. Zhang, W.Y. Li, Y. K. Zhang, *J. Chromatogr. A*, 2009 **1216**, 807.
20 S.L. Lu, G.X. Cheng and X.S. Pang, *J. Appl. Polym. Sci*., 2006, **99**, 2401.
21 L. Qin, X.W. He, W. Zhang, W.Y. Li and Y.K. Zhang, *Anal. Chem*., 2009, **81**, 7206.
22 T.Y. Guo, Y.Q. Xia, G.J. Hao, M.D. Song and B.H. Zhang, *Biomaterials*, 2004, **25**, 5905.
23 G.Q. Fu, H. Yu and J. Zhu, *Biomaterials*, 2008, **29**, 2138.
24 L. Carolyn, E.P.H. Bayer, N.A. Peppas, *J. Biomater. Sci. Polym. Ed.*, 2011, **22**, 1523
25 J.Y. Sun, X.H. Zhao, W.R.K. Illeperuma, O. Chaudhuri, K.H. Oh, D.J. Mooney, J.J. Vlassak and Z.G. Suo, *Nature*, 2012, **489**, 133.
26 K.Y. Zhao, B.B. Lin, W.K. Cui, L.Z. Feng, T. Chen and J.F. Wei, *Talanta*, 2014, **121**, 256.
27 X.S. Pang, G.X. Cheng, Y.H. Zhang and S.L. Lu, *React. Funct. Polym*., 2006, **66**, 1182.
28 K.Y. Zhao, G.X. Cheng, J.J. Huang and X.G. Ying, *React. Funct. Polym*., 2008, **68**, 732.
29 L.Z. Feng, B.H. Kan, K.Y. Zhao, J.F. Wei, D.W. Zhu and L.H. Zhang, *J. Sol-Gel Sci. Techn*., 2014, **71**, 428.
30 K.Y. Zhao, G.X. Cheng, X.G. Ying and L. Chen, *J. Appl. Polym. Sci*., 2009, **113**, 1133.
31 K.Y. Zhao, G.X. Cheng, J.J. Huang and X.G. Ying, *React. Funct. Polym*., 2008, **68**(3): 732.
32 K.Y. Zhao, J.J. Huang, X.G. Ying and G.X. Cheng. *J. Appl. Polym. Sci*., 2008, **109**, 2687.

